Nonradiative Transition of Phosphorescent Charge-Transfer States of Ruthenium(II)-to-2,2′-Biquinoline and Ruthenium(II)-to-2,2′:6′,2″-Terpyridine in the Solid State

Ashraful Islam, Noriaki Ikeda, Akio Yoshimura, and Takeshi Ohno*

Department of Chemistry, Graduate School of Science, Osaka University, 1-16 Machikane-yama, Toyonaka, Osaka 560-0043, Japan

Received February 27, 1997

Temperature-dependent decays of the charge-transfer triplet excited states (^{3}CT) of ruthenium(II) compounds have been investigated in a wide temperature range (77−480 K) for the crystals of $Ru(biq)_3(ClO_4)_2$, $Ru(bpy)_2(biq)X_2 \cdot 2H_2O$, and $Ru(tpy)_2X_2$, (bpy = 2,2′-bipyridine, tpy = 2,2′:6′,2″-terpyridine, biq = 2,2′-biquinoline, X = ClO_4^-, PF_6^-). The width of the ^{1}CT absorption band and the peak of ^{3}CT emission of the $Ru(bpy)_2(biq)X_2 \cdot 2H_2O$ crystal at 298 K are unchanged from those of the ethanol/methanol solution sample. The ^{3}CT of $Ru(bpy)_2(biq)X_2 \cdot 2H_2O$ and $Ru(biq)_3(ClO_4)_2$ in the solid state above 370 K are converted to a higher lying excited state, the d−d triplet lowest excited state (^{3}(d−d)), with a frequency factor of $>10^{13}$ s^{-1} and an activation energy of >3100 cm^{-1}, followed by the rapid degradation of the higher excited state. A small frequency factor ($<10^{12}$ s^{-1}) and an activation energy (<2000 cm^{-1}) of the nonradiative decay of ^{3}CT for $[Ru(tpy)_2]X_2$ in the solid state indicates that the exoergonic intersystem crossing of ^{3}(d−d) to the ground state is the rate-determining process of ^{3}CT decay above 200 K.

Introduction

Polypyridine complexes of Ru(II) in polar solvents emit strong metal-to-ligand charge-transfer (CT) phosphorescence even at room temperature,[1,2] while most d−d emissions of Cr(III)[3,4] and Rh(III)[5] complexes in polar solvent are replaced by ligand-substitution reaction. Shortening of the excited-state lives of various ruthenium(II) compounds at higher temperatures has been ascribed to endoergonic conversion to a higher lying and displaced intermediate such as ^{3}(d−d) state followed by intersystem crossing to the ground state.[6−18] A large activation volume for the nonradiative transition of ^{3}CT in the solution[19] indicated the formation of a displaced intermediate undergoing efficient transition to the ground state. The deformed emission spectra in the solution phase[2,14−18,20−22] suggest that the molecular structure of the excited ruthenium(II) compound is different from that in the ground state.

A kinetic spectroscopic study of ruthenium(II) compounds in the solid state[23] has revealed that (1) $Ru(bpy)_3(PF_6)_2$ exhibits a temperature-independent phosphorescence spectrum in a wide temperature range (77−300 K), and (2) a higher lying and displaced ^{3}(d−d) state with a $d\pi^5 d\sigma^*$ configuration is efficiently formed with a high frequency factor of 7.6×10^{13} s^{-1} and an activation energy of 5200 cm^{-1}. Meanwhile, for ruthenium(II) compounds of a bulky ligand of 2,2′-biquinoline (biq) and a sterically hindered ligand of 2,2′:6′,2″-terpyridine (tpy), the ^{3}(d−d) states were speculated to lie close to ^{3}CT on the basis of the short lives of ^{3}CT at room temperature in solution. The low-energy levels of ^{3}(d−d) states were ascribed to weaker ligand field due to the bulkiness of biq and the steric hindrance of tpy.[11,12,14−17,24,25] The emission decays from ^{3}(d−d) excited states with $d\pi^5 d\sigma^*$ configuration have been intensively studied for Rh(III) compounds in solution[26−29] and in solid state.[30,31]

(1) Kalyanasundaram, K. *Coord. Chem. Rev.* **1982**, *46*, 159.
(2) Juris, A.; Balzani, V.; Barigelletti, F.; Campagna, P.; Belser, P.; von Zelewsky, A. *Coord. Chem. Rev.* **1988**, *84*, 85.
(3) Lessard, R. B.; Endicott, J. F.; Perkovic, M. W.; Ochrymowycz, L. A. *Inorg. Chem.* **1989**, *28*, 2574.
(4) Forster, L. S. *Adv. Photochem.* **1991**, *16*, 215.
(5) Frink, M. E.; Ford, P. C. *Inorg. Chem.* **1985**, *24*, 1033.
(6) (a) Von Houten, J.; Watts, R. *J. Am. Chem. Soc.* **1975**, *97*, 3843. (b) Van Houten, J.; Watts, R. *Inorg. Chem.* **1978**, *17*, 3381.
(7) Malouf, G.; Ford, P. C. *J. Am. Chem. Soc.* **1977**, *99*, 7211.
(8) Allsopp, S. R.; Cox, A.; Kemp, T. J.; Reed, W. J. *J. Chem. Soc., Faraday Trans.* **1978**, *5*, 1275.
(9) Durham, B.; Casper, J. V.; Nagle, J. K.; Meyer, T. J. *J. Am. Chem. Soc.* **1982**, *104*, 4803.
(10) (a) Casper, J. V.; Meyer, T. J. *Inorg. Chem.* **1983**, *22*, 2444. (b) Casper, J. V.; Meyer, T. J. *J. Am. Chem. Soc.* **1983**, *105*, 5583.
(11) Henderson, L.; Fronczek, F. R., Jr.; Cherry, W. R. *J. Am. Chem. Soc.* **1984**, *106*, 5876.
(12) Kirchoff, J. R.; McMillan, D. R.; Marnot, P. A.; Sauvage, J. P. *J. Am. Chem. Soc.* **1985**, *107*, 1138.
(13) Kemp, T. J. *Prog. React. Kinet.* **1980**, *10*, 301.
(14) Barigelletti, F.; Juris, A. Balzani, V.; Belser, P.; von Zelewsky, A. *Inorg. Chem.* **1983**, *22*, 3335.
(15) Juris, A.; Barigelletti, F.; Balzani, V.; Belser, P.; von Zelewsky, A. *Inorg. Chem.* **1985**, *24*, 202.
(16) Barigelletti, F.; Belser, P.; von Zelewsky, A. Balzani, V. *J. Phys. Chem.* **1985**, *89*, 3680.
(17) Barigelletti, F.; Juris, A.; Balzani, V.; Belser, P.; von Zelewsky, A. *J. Phys. Chem.* **1987**, *91*, 1095.
(18) Hager, G. D.; Crosby, G. A. *J. Am. Chem. Soc.* **1975**, *97*, 7031.
(19) Fetterrolf, M. L.; Offen, H. W. *J. Phys. Chem.* **1985**, *89*, 3320.
(20) Ferguson, J.; Krausz, E.; Maeder, M. *J. Phys. Chem.* **1985**, *89*, 1852.
(21) Kitamura, N.; Kim, H.-B.; Kawanishi, Y.; Obata, R.; Tazuke, S. *J. Phys. Chem.* **1986**, *90*, 1468.
(22) Ferguson, J.; Krausz, E. *Chem. Phys. Lett.* **1986**, *127*, 551.
(23) Islam, A.; Ikeda, N.; Nozaki, K.; Ohno, T. *Chem. Phys. Lett.* **1996**, *263*, 209.
(24) Hecker, C. R.; Grushurst, K. I.; McMillin, D. R. *Inorg. Chem.* **1991**, *30*, 538.
(25) Maestri, M.; Armaroli, N.; Balzani, V.; Constable, E. C.; Cargill Thompson, A. M. W. *Inorg. Chem.* **1995**, *34*, 2759.
(26) Sexton, D. A.; Skisted, L. H.; Magde, D.: Ford, P. C. *Inorg. Chem.* **1984**, *23*, 4533.
(27) Skibsted, L. H.; Hancock, M. P.; Magde, D.: Sexton, D. A. *Inorg. Chem.* **1984**, *23*, 3735.

S0020-1669(97)00242-5 CCC: $15.00 © 1998 American Chemical Society
Published on Web 05/27/1998

The preexponential factor of the emission decay ($<10^{12}$ s^{-1}) observed for a crystal of *cis*-[$Rh(bpy)_2Cl_2$](PF_6) was ascribed to a nonadiabatic and highly exoergonic transition of ^{3}(d−d) to the ground state.[31]

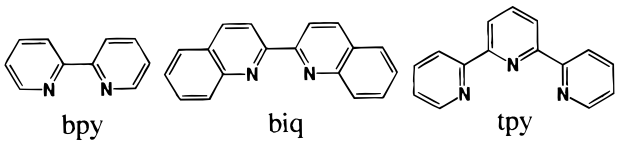

In this paper, the direct verification that the lowest d−d excited state of a $d\pi^5d\sigma^*$ configuration is the intermediate for the rapid nonradiative transition of ^{3}CT is pursued for ruthenium(II) compounds of a bulky ligand of 2,2′-biquinoline (biq) and of a sterically hindered ligand of 2,2′:6′,2″-terpyridine (tpy) in the solid state. The temperature dependency of the nonradiative rate of emission for crystalline compounds of $Ru(biq)_3(ClO_4)_2$, $Ru(bpy)_2(biq)X_2{\cdot}2H_2O$, $Ru(tpy)_2X_2$ ($X = ClO_4^-$ PF_6^-), and $Ru(tpy)_2Cl_2{\cdot}6H_2O$ are examined in a wide temperature range (77−480 K). The preexponential factor of the emission decay process for $Ru(tpy)_2X_2$, ($X = ClO_4^-$, PF_6^-) is compared with those of ^{3}(d−d) of *cis*-[$Rh(bpy)_2Cl_2$]Cl with the same electronic configuration of $d\pi^5d\sigma^*$.

Experimental Section

Materials. $Ru(biq)_3(ClO_4)_2$,[32] $Ru(bpy)_2(biq)X_2{\cdot}2H_2O$ ($X = ClO_4^-$, PF_6^-),[33] $Ru(tpy)_2Cl_2{\cdot}6H_2O$[34] were synthesized and purified according to the literature methods. For $Ru(tpy)_2X_2$, the counterions were changed by adding $NaClO_4$ or NH_4PF_6 solution to the corresponding chloride complex. $RuCl_3{\cdot}3H_2O$ and all ligands were purchased commercially and used without further purification. Data of elementary analysis for the complexes are in the agreement with those calculated. Emission spectra of the compounds were measured on excitation of a crystalline or microcrystalline form after recrystallization. But some anhydrous complexes showed nonexponential decay, and they were recrystallized several times until single-exponential decay was obtained. The lifetimes measured were not affected by the size of the crystal. A transparent disc with a diameter of 10 mm and thickness of 1 mm was prepared for the measurement of absorption spectrum in the following way. The ground microcrystal of an Ru(II) compound (1 mg) was dispersed in ground KCl (2 g). The ground mixture (120 mg) was pressed to be transparent under vacuum. An island of the red crystal was invisible under magnification.

Apparatus and Measurements. The emission spectra were measured by using a grating monochromator (Jasco CT250) with a silicon diode array (Hamamatsu S3901-512Q). The 488 line of an Ar laser (Coherent Innova 306) was used for the excitation of crystal samples. The sensitivity of emission measurement was corrected by using a bromine lamp (Ushio JPD100V500WCS). The apparatus for the measurement of emission decay rate was described elsewhere.[35] The excitation laser intensity was attenuated to less than about 1μJ/pulse by neutral density filters to avoid nonlinear photoprocesses such as triplet−triplet annihilation.[35] The decay rates were determined by a least-squares fit to the single-exponential decay. The sample crystals on a copper holder were retained in a cryostat (Oxford DN1740) controlled by an Oxford ITC4 controller in the temperature range of 77−300 K. The samples in a capillary Pyrex cell were put in a circulating water bath (Neslab RTE-B5) between 300 and 350 K and into an aluminum block and heated by a hot plate between 350 and 480 K. Thermoanalytical measurements of $Ru(bpy)_2(biq)X_2{\cdot}2H_2O$ ($X = ClO_4^-$, PF_6^-) were performed using a calorimeter (Seiko TG/DTA-200).

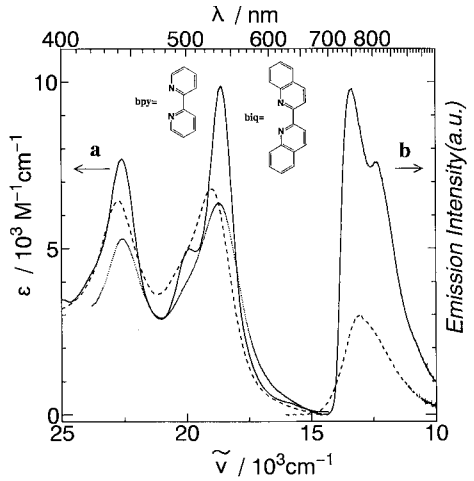

Figure 1. Absorption and emission spectra of $Ru(bpy)_2(biq)(PF_6)_2{\cdot}2H_2O$. (a) Absorption spectra of the crystal dispersed in a transparent KCl disc at room temperature (···) and of the ethanol/methanol (3:1) solution at room temperature (- - -) and 77 K (—), (b) emission spectra of the crystalline solid at room temperature (- - -) and 77 K (—).

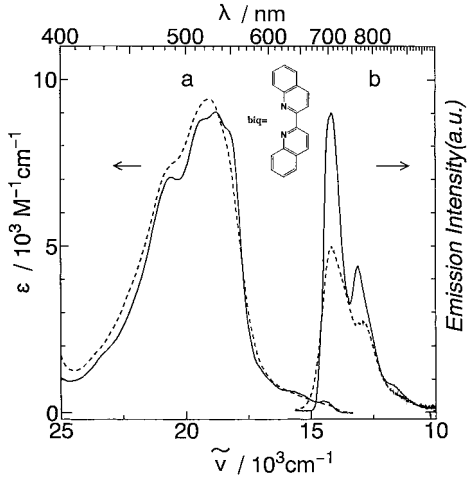

Figure 2. Absorption and emission spectra of $Ru(biq)_3(ClO_4)_2$ at room temperature (···) and at 77 K (—). (a) Absorption spectra in ethanol−methanol (3:1). (b) Emission spectra of the crystalline solid.

Results

Absorption and Emission Spectra. Absorption spectra of microcrystalline $Ru(bpy)_2(biq)X_2{\cdot}2H_2O$ dispersed in a transparent KCl disc at 298 K and the ethanol/methanol sample are shown in Figure 1. The peak energy of the strongest bands of the crystal in KCl disc at 298 K were identical to those of the ethanol/methanol solution at 77 K. The half-width at half-maximum of the strongest band was 900 cm^{-1} for both the crystal in the KCl disc and the solution at 298 K. Absorption spectra of $[Ru(biq)_3](PF_6)_2$ and $[Ru(tpy)_2]X_2$ in ethanol/methanol (3:1 by volume) at 77 K are shown in Figures 2 and 3. Raising the temperature brought no shift of the absorption peaks.

Every crystal studied here exhibited a structured emission at 77 and 298 K as shown in Figures 1−3. When the raising temperature is increased, the highest-energy part of emission was weakened with a small shift to the lower energy. The deformation of the emission at room temperature is ascribed to

(28) Ohno, T.; Kato, S. *Bull. Chem. Soc. Jpn*. **1984**, *57*, 3391.
(29) Nishizawa, M.; Suzuki, T. M.; Sprouse, S. D.; Watts, R. J.; Ford, P. C. *Inorg. Chem.* **1984**, *23*, 1837.
(30) Weaver, S. C.; McClure, D. S. *Inorg. Chem*. **1992**, *31*, 2814.
(31) Islam, A.; Ikeda, N.; Nozaki, K.; Ohno, T. *Photochem. Photobiol. A: Chem*. **1997**, *106*, 61.
(32) Klassen, D. M. *Inorg. Chem*. **1976**, *15*, 3166.
(33) Belser, P. *Helv. Chim. Acta* **1980**, *23*, 1675.
(34) Palmer, R. A.; Piper, T. S. *Inorg. Chem*. **1966**, *5*, 864.
(35) Iguro, T.; Ikeda, N.; Ohno, T. *Inorg. Chim. Acta* **1994**, *226*, 203.

Table 1. Energies, Lifetimes, and Decay Parameters of Emissions of Ru(II) Salts in Crystal

crystal	$\bar{\nu}_{max}$/cm^{-1} 77 K	τ/μs ~298 K	τ/μs 77 K	$k_L/10^5$ s^{-1}	E_L/cm^{-1}	$k_M/10^5$ s^{-1}	E_M/cm^{-1}	$k_H/10^{13}$ s^{-1}	E_H/cm^{-1}
$Ru(bpy)_2(biq)(ClO_4)_2 \cdot 2H_2O$	13 100	0.20	0.50	50	48	500	750	30	5500
$Ru(bpy)_2(biq)(PF_6)_2 \cdot 2H_2O$	13 400	0.22	0.67	40	56	160	520	6	4800
					30[a]		600[a]		
$Ru(bpy)_2(biq)(PF_6)_2$ [b]				20	48	80	300	0.16	3600
$Ru(biq)_3(ClO_4)_2$	14 200	0.17	2.4	20	70			1	3100
$Ru(tpy)_2(ClO_4)_2$	16 500	<0.01	5.0	6.2	64			0.02	1100
$Ru(tpy)_2(PF_6)_2$	16 100	~0.01	6.7	6.2	80			0.11	2000
$Ru(tpy)_2Cl_2 \cdot 6H_2O$	16 400	0.01	5.8	5.1	64			0.02	1700

[a] From the measurement of emission intensity. [b] Obtained by the dehydration of $Ru(bpy)_2(biq)(PF_6)_2 \cdot 2H_2O$ at 370 K.

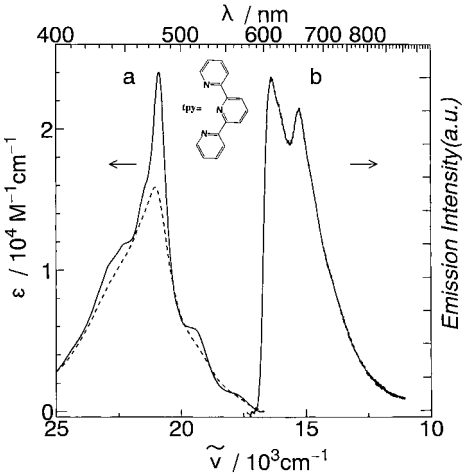

Figure 3. Absorption and emission spectra of $Ru(tpy)_2Cl_2 \cdot 6H_2O$. (a) Absorption spectra in ethanol−methanol (3:1) at room temperature (···) and at 77 K(−). (b) Emission spectrum of the crystalline solid at 77 K.

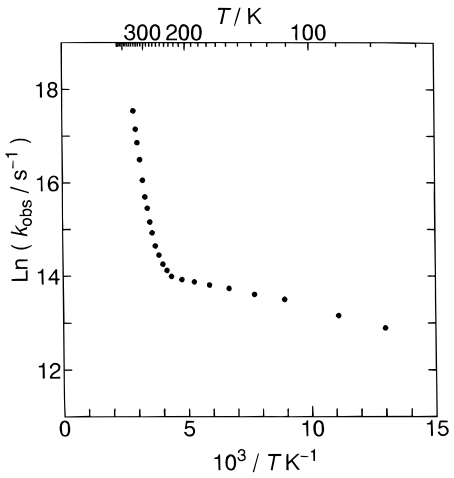

Figure 4. Temperature dependence of the emission decay rate (k_{obs}) for the $Ru(biq)_3(ClO_4)_2$ crystal.

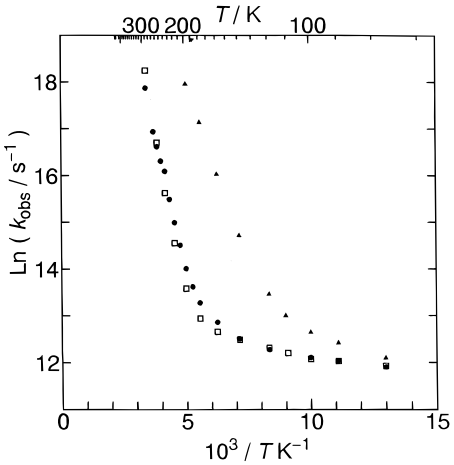

Figure 5. Temperature dependence of the emission decay rate (k_{obs}) for $Ru(tpy)_2Cl_2 \cdot 6H_2O$ (●), $Ru(tpy)_2(PF_6)_2$ (□), and $Ru(tpy)_2(ClO_4)_2$ (▲) crystals.

reabsorption,[23,35,36] because the intensity of the highest energy band was recovered on monitoring the emission from the front surface of the single crystal. $Ru(biq)_3(ClO_4)_2$ and $Ru(bpy)_2(biq)X_2 \cdot 2H_2O$ at 77 and 298 K exhibit one emission with a peak at 14 200 and 13 100−13 400 cm^{-1}, respectively, with a temperature-dependent full-width at half-maximum.

Temperature-Dependent Decay of Emission. All emissions of the crystalline samples decay via a single-exponential mode over a wide temperature range (77−480 K). The lifetimes of crystalline $Ru(bpy)_2(biq)X_2 \cdot 2H_2O$ at 77 K are a little shorter (0.5−0.67 μs) than those of the rigid solution (Table 1). Emission lifetimes of crystalline $Ru(tpy)_2Cl_2 \cdot 6H_2O$ and $Ru(tpy)_2(PF_6)_2$ at room temperature are much longer (10 ns) than that of the solution sample (0.025 ns).[37] Figures 4−6 show the temperature dependence of emission decay rates for the ruthenium(II) compounds studied. Below 200 K the decay rates of emission are weakly dependent on temperature. Above 200 K the decay rate of emission increased with temperature. The emission decays of $Ru(biq)_3(ClO_4)_2$ (Figure 4) and $Ru(tpy)_2X_2$ (Figure 5) were analyzed following to an Arrhenius-type equation (eq 1)

$$k_{obs}(T) = k_L \exp(-E_L/RT) + k_H \exp(-E_H/RT) \qquad (1)$$

where k_L, E_L and k_H, E_H stand for the preexponential factor and the activation energy of emission decay dominating in the low- and high-temperature regions, respectively.

As for $Ru(bpy)_2(biq)X_2 \cdot 2H_2O$ (X = PF_6^-, ClO_4^-), the emission decay was more dependent on temperature in the range of 350−480 K (Figure 6). Emission of $Ru(bpy)_2(biq)X_2 \cdot 2H_2O$ decays via three modes, and the decay rate of emission can be expressed in eq 2

$$k_{obs}(T) = k_L \exp(-E_L/RT) + k_M \exp(-E_M/RT) + k_H \exp(-E_H/RT) \qquad (2)$$

where k_M and E_M stand for the preexponential factor and the

(36) Yersin, H.; Hensler, G.; Gallhuber, E. *Inorg. Chim. Acta* **1987**, *132*, 187.
(37) Winkler, J. R.; Netzel, T. L.; Creutz, C.; Sutin, N. *J. Am. Chem. Soc.* **1987**, *109*, 2381.

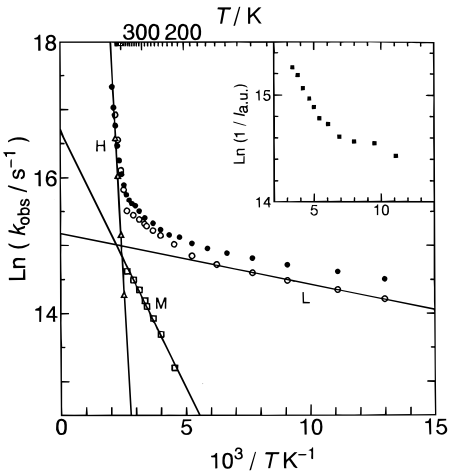

Figure 6. Temperature dependence of the decay rate (k_{obs}) of the emission for $Ru(bpy)_2(biq)(PF_6)_2 \cdot 2H_2O$ (○) and $Ru(bpy)_2(biq)(ClO_4)_2 \cdot 2H_2O$ (●) crystals. The lines, L, M, and H, represent the fits to eq 2 for the low-, medium-, and high-temperature processes for $Ru(bpy)_2(biq)(PF_6)_2 \cdot 2H_2O$. The corrected data (□, △) were obtained by subtracting the contribution of the lower-temperature decay channels. The inset shows the temperature dependence of emission intensity (I) of $Ru(bpy)_2(biq)(PF_6)_2 \cdot 2H_2O$.

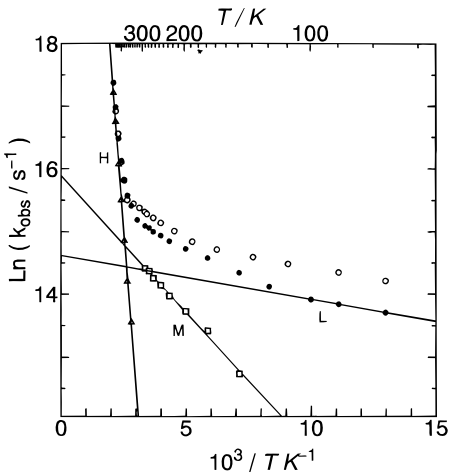

Figure 7. Temperature dependence of the emission decay rate (k_{obs}) for the dehydrated (●) and hydrated (○) crystals of $Ru(bpy)_2(biq)(PF_6)_2 \cdot 2H_2O$. The lines, L, M, and H, represent the fits to eq 2 for the low-, medium-, and high-temperature decay channels for the dehydrated crystal. The corrected data (□, △) were obtained by subtracting the contribution of the lower-temperature region.

activation energy of the emission decay in the middle temperature region of 180−350 K, respectively. Parameters for the medium- and high-temperature processes were obtained by subtracting the contribution of the lower-temperature process. All the activation energies and the preexponential factors for the above compounds are shown in Table 1.

Discussion

Absorption and Emission Spectra. The absorption peaks at 18 900 and 22 600 cm^{-1} of both the crystals dispersed in a transparent KCl disc and the ethanol/methanol solution of $Ru(bpy)_2(biq)(PF_6)_2 \cdot 2H_2O$ at 298 K are ascribed to Ru-to-biq CT and Ru-to-bpy CT, respectively. No broadening of the CT absorption bands demonstrates that no molecular interactions split the CT excited state much in the solid state. The peak shift of the solution sample with temperature suggests the existence of solvent reorganization on the photoexcitation at high temperature. A broad absorption band of $Ru(biq)_3^{2+}$ with small peaks in the 18 200−20 800 cm^{-1} region are ascribed to the Ru-to-biq CT bands. The solution of $Ru(tpy)_2^{2+}$ displays a single absorption peak at 20 800 cm^{-1} with longer wavelength shoulders, which can be assigned to Ru-to-tpy CT.

The emission peak energy of the crystalline sample at 77−300 K is quite similar to that of the solution sample at 77 K. Absence of the emission peak shift with temperature implies that the ^{3}CT of the crystalline compounds are not deformed in the wide temperature range. The energy of ^{3}CT emission decreases in the following order: $[Ru(tpy)_2X]_2 > [Ru(biq)_3](PF_6)_2 > [Ru(bpy)_2(biq)](PF_6)_2$.

Decay of Emission. An Arrhenius-type temperature dependence of the emission decay reveals the presence of two decay modes for $[Ru(biq)_3](PF_6)_2$ and $[Ru(tpy)_2](PF_6)_2$ and three decay modes for $[Ru(bpy)_2(biq)](PF_6)_2$ in a wide temperature range. A large difference in the magnitude of preexponential factors and activation energy between the low-temperature channel and the high-temperature channel affords the accuracy in the determination of k_H and E_H.

Low-Temperature Decay Channels. A decay mode with E_L (<100 cm^{-1}) and k_L (10^6 s^{-1}) is predominant in the low-temperature region of 77−200 K for $[Ru(bpy)_2(biq)]X_2 \cdot 2H_2O$ (Figure 6) and $[Ru(biq)_3](ClO_4)_2$ (Figure 4) in the solid state. A decay mode with E_L (<100 cm^{-1}) and k_L (10^5 s^{-1}) is predominant below 110 K for $[Ru(tpy)_2](ClO_4)_2$ and below 160 K for $[Ru(tpy)_2](PF_6)_2$ and $[Ru(tpy)_2]Cl_2 \cdot 6H_2O$ in the solid state (Figure 5). The low activations (E_L < 100 cm^{-1}) of the emission decay are ascribed to the population of ^{3}CT states lying 61 cm^{-1} higher than the lowest one, as has been verified for $[Ru(bpy)_3](PF_6)_2$ below 20 K.[38] Since the lifetimes of the emission are long enough to establish an equilibrium between closely lying ^{3}CT states, the preexponential factor of the higher lying ^{3}CT is estimated to be 10^6 s^{-1}. The magnitude of E_L corresponds to the Gibbs energy change of the higher ^{3}CT state. The high-temperature channel began to emerge around 100 K exceptionally for $Ru(tpy)_2(ClO_4)_2$, so that the k_L and E_L of the low-temperature decay channel are not so accurate.

Medium-Temperature Decay Channels. The medium-temperature channel of decay for $[Ru(bpy)_2(biq)]X_2 \cdot 2H_2O$ was clearly observed in a temperature range of 180−370 K. The presence of the medium-temperature decay channel is distinctly seen on plotting ln $1/I_p$ (I_p is the emission intensity) versus $1/T$. Since the magnitude of the slope is close to that of E_M/R obtained for plotting ln k versus $1/T$, the enhanced decay of emission is ascribed to a nonradiative transition of ^{3}CT via an upper ^{3}CT.[14,39] A small magnitude of the preexponential factor (10^7 s^{-1}) implies that the mechanism of the nonradiative transition is different from that seen in the high-temperature region (vide infra).

Dehydration of the crystal in the temperature region of 300−370 K was detected to occur by means of thermogravimetry and differential thermal analysis. The decay rates between 300 and 370 K were observed for the partially dehydrated crystal. The completely dehydration, which occurred above 370 K, reduced the decay rate a little in the temperature range of 180−300 K, as is shown in Figure 7. However, there was an emission decay channel left for the dehydrated crystal of $[Ru(bpy)_2(biq)](PF_6)_2$ in the low-temperature region. The magnitudes of A_M and E_M are of the same order as those for the hydrated crystal. Therefore, the presence of solvated water is not responsible for the second decay channel in a 180−370 K region of temperature.

(38) Yersin, H.; Braun, D. *Chem. Phys. Lett.* **1991**, *179*, 85.
(39) Lumpkin, R. S.; Kober, E. M.; Worl, L. A.; Murtaza, Z.; Meyer, T. J. *J. Phys. Chem.* **1990**, *94*, 239.

Scheme of the High-Temperature Decay Channel. It has been proposed that an excited ^{3}(d−d) state in the solid state is involved in the efficient decay channel of ^{3}CT in the high-temperature region of $[Ru(bpy)_3](PF_6)_2$.[23] The efficient nonradiative transition of ^{3}CT occurs via the following sequential process

$$^3\text{MLCT} \xrightarrow{k_{12}} {}^3(\text{d}-\text{d}) \xrightarrow{k_{20}} \text{singlet ground state} \qquad (3)$$

where the first internal conversion with a rate constant of k_{12} and the second intersystem crossing with a rate constant of k_{20} are endoergonic and heavily exoergonic, respectively. The ^{3}(d−d) state with an electronic configuration of $d\pi^5 d\sigma^*$ is inferred to be well displaced. Quite broad phosphorescences from ^{3}(d−d) of Rh(III) compounds such as $Rh(NH_3)_5X^{2+}$ [40] and *cis*-$Rh(bpy)_2X_2^+$ [31,41] demonstrate that the ^{3}(d−d) state is well displaced. The displacement of the potential curve of ^{3}(d−d) with respect to both the ^{3}CT and the ground state makes both the internal conversion and the intersystem crossing so efficient. Because of the ergonicity, the internal conversion process is the rate-determining step of the rapid nonradiative transition. The rate of endoergonic formation of ^{3}(d−d) can be written to the first-order approximation in terms of the ergonicity ($\Delta G_{12}°$) and the reorganization energy (λ_{12}) of ^{3}(d−d) formation as follows:

$$k_{12} = \omega \exp\left(-\frac{(\Delta G_{12}° + \lambda_{12})^2}{4\lambda_{12} k_B T}\right) \qquad (4)$$

where ω is the effective frequency of internal conversion. The reorganization energy of ^{3}(d−d) formation from the ground state is estimated for Rh(III) compounds based on the Franck−Condon energy (E_{FC}^{dd}) of d−d emission. The extent of E_{FC}^{dd} is 6400 cm^{-1} at 300 K for the ^{3}(d−d) state of a Rh(III) compound, *cis*-$[Rh(bpy)_2Cl_2](PF_6)$, in the solid.[31] The Franck−Condon energy of ^{3}CT emission of Ru(II) compounds (E_{FC}^{CT}) is less than 1000 cm^{-1} for $Ru(bpy)_3(PF_6)_2$[44] so that λ_{12} for the internal conversion, $^3\text{CT} \rightarrow {}^3$(d−d), is assumed to be 5400 cm^{-1} ($E_{FC}^{dd} - E_{FC}^{CT}$) ∼ 7400 cm^{-1} ($E_{FC}^{dd} + E_{FC}^{CT}$).

Meanwhile, the highly exoergonic intersystem crossing of a displaced ^{3}(d−d) excited state can occur via two processes; the first one takes place adiabatically, and the second one takes place nonadiabatically. The rate of the exoergonic intersystem crossing (k_{20}) can be written in terms of the ergonicity ($\Delta G_{20}°$), the reorganization energy (λ_{20}), the frequency (ν), the quantum number (n), and the Huang−Rhys factor (S) of an accepting vibrational mode and vibronic coupling matrix element (H_{if}), as has been used for the estimation of exoergonic electron-transfer rates.[42]

$$k_{20} = \frac{4\pi^2 H_{if}^{\,2}}{h\sqrt{4\pi\lambda_{20} k_B T}} \sum_{n=0} e^{-s}\frac{S^n}{n!} \exp\left(-\frac{(\Delta G_{20}° + nh\nu + \lambda_{20})^2}{4\lambda_{20} k_B T}\right) \qquad (5)$$

Since the nonadiabatic transition to the vibrational excited state of the ground state needs no thermal energy, the rate of the nonadiabatic process is independent of temperature and the extent of E_H and k_H are reduced as a result in comparison with the adiabatic process.

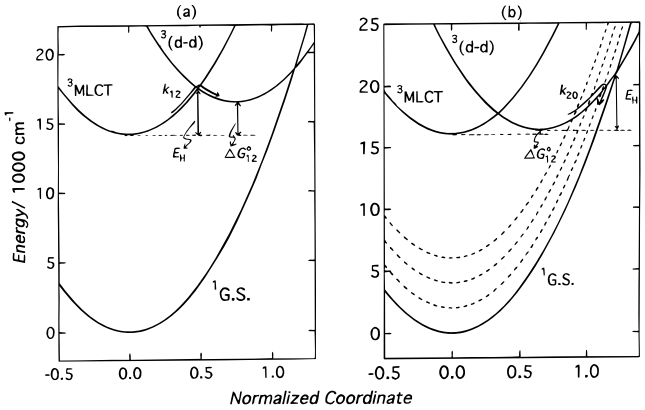

Figure 8. Schemes of nonradiative decay pathways of ^{3}MLCT for (a) $Ru(biq)_3(ClO_4)_2$ and (b) $Ru(tpy)_2(PF_6)_2$. ^{1}G.S. indicates the ground state (−) and vibrationally excited ground state (- - -).

An alternative scheme of the rapid nonradiative decay of ^{3}CT is the quenching of an excited state thermally populated from ^{3}CT by unknown impurities (or defect of crystal). The unknown impurities quench a higher lying excited state with a rate of $10^{12}-10^{14}$ s^{-1}, which is the preexponential factor of the decay process in the high-temperature region. One candidate of the higher excited state is ^{1}CT, which could migrate to meet the quencher within $10^{-12}-10^{-14}$ s^{-1}, if the dipole−dipole interaction is so strong that the singlet exciton state is generated. If the formation of ^{1}CT followed by the rapid quenching is the rate-determining step of the ^{3}CT-quenching, the activation energy of the singlet exciton formation should be in agreement with the ^{1}CT−^{3}CT energy gap. The activation energy of the fast decay process will be a reliable diagnosis for the higher excited state involved in the quenching. Another important issue is the preexponential factor of the nonradiative process obtained by extrapolation, which can be proportional to the diffusion constant of exciton and the mole fraction of quenchers. If the diffusion constant of the exciton migration is fairly large ($>10^{-2}$ cm^2 s^{-1}), a quencher of 10^{-3} mol/mol is capable to meet the exciton within $10^{-12}-10^{-14}$ s.[43] This might not be the case, however, because a large exciton splitting of ^{1}CT absorption band has not been observed for $[Ru(bpy)_2(biq)](PF_6)$.

$Ru(biq)_3(ClO_4)_2$ and $Ru(bpy)_2(biq)X_2{\cdot}2H_2O$ ($X = PF_6^-$, ClO_4^-). The dehydrated crystal of $Ru(bpy)_2(biq)X_2{\cdot}2H_2O$ exhibited a sharp rise of the nonradiative transition via the high-temperature decay mode above 350 K for $X = PF_6^-$ (see Figure 7) and above 370 K for $X = ClO_4^-$, respectively. The rapid nonradiative decay of $^3Ru(bpy)_2(biq)^{2+}$ in the solution above 350 K was not detected because of the short phosphorescence lifetime.[14] The magnitude of k_H at the high-temperature limit is $(6-30) \times 10^{13}$ s^{-1} for $[Ru(bpy)_2(biq)]X_2$ ($X = PF_6^-$, ClO_4^-). The similar magnitude of k_H to a frequency of molecular vibration can be ascribed to an endoergonic internal conversion to a displaced ^{3}(d−d) state as is shown in Figure 8a.

The large magnitude of E_H (4800−5500 cm^{-1}) for the dehydrated crystal of $[Ru(bpy)_2(biq)]X_2{\cdot}2H_2O$ ($X = PF_6^-$,

(40) Thomas, T. R.; Crosby, G. A. *J. Mol. Spectrosc.* **1971**, *38*, 118.
(41) Carstern, H. W.; Crosby, G. A. *J. Mol. Spectrosc.* **1970**, *34*, 113.
(42) Ulstrup, J.; Jortner, J. *J. Chem. Phys.* **1975**, *63*, 4358.
(43) Microcrystals of $[Ru(biq)_3](ClO_4)_2$ dispersed in a transparent disc of KCl exhibited annihilation of ^{3}CT on the high-power laser excitation. The second-order rate constant of annihilation was estimated to be 10^8 M^{-1} s^{-1} from the emission decay and the production of ^{3}CT, which was measured by means of transient absorption.[44] The diffusion constant of ^{3}CT exciton is estimated less than 10^{-7} cm^2 s^{-1} from the annihilation rate constant so that 10% of the ^{3}CT is quenched without any migration by impurity of 10^{-3} mol/mol and the rest of ^{3}CT decays exponentially. Since the biphasic decay of ^{3}CT is not the case, the presence of impurity (10^{-3} mol/mol) can be excluded for the crystal.
(44) Yoshimura, A.; Ohno, T. To be submitted.

Table 2. Rate of the Formation ($k_{12}°$) or Decay ($k_{20}°$) of an Intermediate for the Radiationless Transition at the High-Temperature Limit, the Gibbs Energy Change of the ^{3}(d−d) formation ($\Delta G_{12}°$), and the Energy Levels of ^{3}MLCT and the Lowest ^{3}(d−d)

crystal	$k_{12}°$ or $k_{20}°$ ($\times 10^{13}$ s^{-1})	$\Delta G_{12}°$ ($\times 10^3$ cm^{-1})	$E(^3\text{MLCT})$ ($\times 10^3$ cm^{-1})	$E(^3(\text{d−d}))^a$ ($\times 10^3$ cm^{-1})
$Ru(bpy)_3(ClO_4)_2$[b]	1.5[c]	4.6 ± 0.2[c]	17.2	21.8 ± 0.2
$Ru(bpy)_2(biq)(ClO_4)_2 \cdot 2H_2O$	30[c]	5.4 ± 0.2[c]	13.1	18.5 ± 0.2
$Ru(bpy)_2(biq)(PF_6)_2 \cdot 2H_2O$	6[c]	4.6 ± 0.2[c]	13.4	18.0 ± 0.2
$Ru(biq)_3(ClO_4)_2$	1[c]	2.5 ± 0.3[c]	14.2	16.7 ± 0.3
$Ru(tpy)_2(ClO_4)_2$	0.02[d]	<0.5	16.5	<17.0
$Ru(tpy)_2(PF_6)_2$	0.11[d]	<0.5	16.1	<16.6

[a] The intermediate is presumed to be ^{3}(d−d). [b] Reference 23. [c] Equation 4 is presumed to assess both $k_{12}°$ and $\Delta G_{12}°$ based on A_H and E_H. [d] Equation 4 is presumed to assess $k_{20}°$ based on A_H and E_H.

ClO_4^-) is close to the ^{1}CT−^{3}CT energy gap (5100−5400 cm^{-1}). The latter is estimated from the difference between the strong absorption peak and the emission peak. The E_H for the anhydrous crystal of $[Ru(biq)_3](ClO_4)_2$ is, however, lower by 900 cm^{-1} than the ^{1}CT−^{3}CT energy gap (4000 cm^{-1}). The mismatch between the E_H and the ^{1}CT−^{3}CT energy gap demonstrates that the ^{1}CT are not involved in the fast decay. The reduction in the activation energy seems to be accounted for in terms of the rapid radiationless decay via ^{3}(d−d). The magnitude of E_H can be related to the ^{3}CT−^{3}(d−d) energy gap ($\Delta G_{12}°$), as eq 4 shows. The magnitude of $\Delta G_{12}°$ is estimated as (2.2−2.8) × 10^3, (4.2−4.8) × 10^3, and (5.2−5.4) × 10^3 cm^{-1} for $[Ru(biq)_3](ClO_4)_2$, $[Ru(bpy)_2(biq)](PF_6)_2$, and $[Ru(bpy)_2(biq)](ClO_4)_2$, respectively, by using eq 4 and λ_{12} (5400−7400 cm^{-1}) (see Table 2). From $\Delta G_{12}°$ and the peak energy of emission, the energy levels of ^{3}(d−d) are estimated to be (16.7 ± 0.3) × 10^3 cm^{-1} and (18.4 ± 0.2) × 10^3 cm^{-1} for $[Ru(biq)_3](ClO_4)_2$ and $[Ru(bpy)_2(biq)](ClO_4)_2$, respectively, which are lower than that of $[Ru(bpy)_3](ClO_4)_2$ ((21.8 ± 0.2) × 10^3 cm^{-1}).[23] The decreasing energy level of ^{3}(d−d) as the number of 2,2′-biquinoline can be understood in terms of the weak ligand-field of 2,2′-biquinoline. Barigelletti et al. presumed that the bond length of Ru−N(biq) are longer than that of Ru−N(bpy) because the bulky biq ligands repel each other.[14] Likewise, repulsion between 2,2′-biquinoline and 2,2′-bipyridine of $[Ru(bpy)_2(biq)](ClO_4)_2$ make the bond lengths of Ru−N(bpy) longer than those of $[Ru(bpy)_3](PF_6)_2$. The longer bond lengths lower the energy levels of ^{3}(d−d) of $[Ru(biq)_3](ClO_4)_2$ and $[Ru(bpy)_2(biq)](ClO_4)$ compared with $[Ru(bpy)_3](ClO_4)_2$.

$[Ru(tpy)_2]X_2$ (X = PF_6^-, ClO_4^-). The activation energy of the fast decay process (1100−2000 cm^{-1}) is smaller than the ^{1}CT−^{3}CT energy gap (2600−4500 cm^{-1}). It demonstrates that ^{1}CT is not involved in the fast decay. The ^{3}CT−^{3}(d−d) energy gap ($\Delta G_{12}°$) is calculated to be smaller than 500 cm^{-1} from the activation energy and the reorganization energy by using eq 4. The low-energy level (16 600−17 000 cm^{-1}) of ^{3}(d−d) of $[Ru(tpy)_2]X_2$ can be ascribed to the longer Ru−N bonds as follows. X-ray diffraction[45] revealed that $[Ru(tpy')_2]X_2$ (tpy′ = 4′-*N*,*N*-dimethylamino-tpy) displays a deformed structure arising from the inability of the tridentate ligands (tpy′) to span 180°, in which the terminal Ru−N bonds are longer than the central Ru−N bond. The low-energy level of the ^{3}(d−d) state for the tpy compound compared with the bpy compound was met for Rh(III) compounds.[46]

Since the ^{3}(d−d) lies rather near to ^{3}CT, the internal conversion of ^{3}CT → ^{3}(d−d) is not the rate-determining step of the radiationless transition any more. The magnitude of k_H, (0.02−0.11) × 10^{13} s^{-1}, is much smaller than those (1 × 10^{13} to 30 × 10^{13} s^{-1}) observed for the endoergonic conversion of ^{3}CT → ^{3}(d−d) in the solid state of $[Ru(bpy)_3](ClO_4)_2$,[34] $[Ru(bpy)_2(biq)](ClO_4)_2$, and $[Ru(biq)_3](ClO_4)_2$. The small magnitude of k_H observed for $[Ru(tpy)_2]X_2$ can be ascribed to an exoergonic intersystem crossing of ^{3}(d−d) to the singlet ground state. In the highly exoergonic processes, the intersystem crossing of a displaced ^{3}(d−d) could occur via two paths: one is an adiabatic path to the ground state, and the other is a nonadiabatical path producing the vibrationally excited ones of the ground state as Figure 8b shows. The nonadiabatic transition to the vibrationally excited state might give rise to smaller extent of activation energy and preexponential factor. A small preexponential factor (<0.7 × 10^{12} s^{-1}) was observed for the intersystem crossing of displaced ^{3}(d−d) states of *cis*-$[Rh(bpy)_2Cl_2](PF_6)$ and *cis*-$[Rh(phen)_2Cl_2](PF_6)$ in the solid state,[34] which has the same electronic configuration of $d\pi^5 d\sigma^*$ as those of the Ru(II) compounds. The spin conversion of ^{3}(d−d) may be partly responsible for the small magnitude of k_{20} in comparison with the internal conversion rate, ^{3}CT → ^{3}(d−d), k_{12}.

Conclusion

The nonradiative decay processes of ^{3}CT exhibiting a temperature-independent emission spectrum were studied over a wide temperature range in the solid state. The ^{3}CT of $[Ru(biq)_3](PF_6)_2$ and $[Ru(bpy)_2(biq)](PF_6)_2 \cdot 2H_2O$ in the high-temperature region undergo endoergonic internal conversion to a highly lying excited state, probably ^{3}(d−d) state, with k_H > 1 × 10^{13} s^{-1} and E_H > 3100 cm^{-1}. The energy levels of ^{3}(d−d) are estimated to be (16.7−18.4) × 10^3 cm^{-1} from the magnitude of E_H and the energy level of ^{3}CT by assuming a large value of the reorganization energy for the ^{3}(d−d) formation. The nonradiative decay of ^{3}CT of $[Ru(tpy)_2]X_2$ occurs with a small preexponential factor of <10^{12} s^{-1}, which can be ascribed to the exoergonic intersystem crossing of ^{3}(d−d) lying close to ^{3}CT.

Acknowledgment. We thank Prof. Y. Kushi and Dr. T. Kawamoto for the use of a calorimeter. The authors wish to thank Dr. F. Barigelletti for giving comments on the manuscript. The present work was partially supported by Grants-in-Aid from the Japanese Ministry of Education, Science, Sports and Culture to N.I. (06640722) and T.O. (06239101).

IC9702429

(45) Constable, E, C,; Cargill Thompson, A. M. W.; Tocher, D. A.; Daniels, M. A. M. *New J. Chem.* **1992**, *16*, 855.
(46) Frink, M. E.; Sprouse, S. D.; Goodwin, H. A.; Watts, R. J.; Ford, P. C. *Inorg. Chem.* **1988**, *27*, 1283.